Wind and Structures, *Vol. 29, No. 4 (2019) 235-246*
DOI: https://doi.org/10.12989/was.2019.29.4.235

Characteristics of wind loading on internal surface and its effect on wind-induced responses of a super-large natural-draught cooling tower

Yun-feng Zou[1,2a], Zheng-yi Fu[1,2b], Xu-hui He*[1,2], Hai-quan Jing**[1,2], Ling-yao Li[1,2c], Hua-wei Niu[3d] and Zheng-qing Chen[3e]

[1]*School of Civil Engineering, Central South University, Changsha, 410075, China*
[2]*National Engineering Laboratory for High Speed Railway Construction, Changsha, 410075, China*
[3]*Wind Engineering Research Center, Hunan University, Changsha, 410082, China*

(Received August 11, 2018, Revised April 11, 2019, Accepted April 26, 2019)

Abstract. Wind loading is one of important loadings that should be considered in the design of large hyperbolic natural-draught cooling towers. Both external and internal surfaces of cooling tower are under the action of wind loading for cooling circulating water. In the previous studies, the wind loads on the external surface attracted concernedly attention, while the study on the internal surface was relatively ware. In the present study, the wind pressure on the internal surface of a 220 m high cooling tower is measured through wind tunnel testing, and the effect of ventilation rate of the packing layer on internal pressure is a major concern. The characteristics of internal wind pressure distribution and its effect on wind-induced responses calculated by finite element method are investigated. The results indicate that the wind loading on internal surface of the cooling tower behaves remarkable three-dimensional effect, and the pressure coefficient varies along both of height and circumferential directions. The non-uniformity is particularly strong during the construction stage. Analysis results of the effect of internal pressure on wind-induced responses show that the size and distribution characteristics of internal pressure will have some influence on wind-induced response, however, the outer pressure plays a dominant role in the wind-induced response of cooling tower, and the contribution of internal pressure to the response is small.

Keywords: cooling tower; internal wind pressure; wind loading; wind tunnel test; wind-induced response

1. Introduction

Natural-draught cooling towers are high-rise structures with a large body, light weight, hyperboloidal shell shape, and low ratio of thickness to radial dimension. They are sensitive to wind and show large response even damages under the wind loading (Niemann et al. 1986, Hashish *et al*. 1974, Bamu *et al*. 2005, Zhao *et al*. 2010, Ke *et al*. 2012, Karakas *et al*. 2016, Zou *et al*. 2018). On November 7, 1965, three out of a group of eight reinforced-concrete cooling towers were blown down in strong wind (wind speed ranging from 33.99 to 37.57 m/s) at Ferrybridge Power Station in Yorkshire county of the UK (CEGB, 1965). Since then, the wind loading and wind-induced response of the cooling towers have attracted considerable attention (Zhang *et al*. 2013, Zhao *et al*. 2017, Cheng *et al*. 2017, Ke *et al*. 2017b). The shell of cooling tower is usually supported by a number of circular columns at the bottom and keeps open at the top to allow wind pass through to cooling the circulating water. Thus, both the external and internal surfaces of the cooling tower are always under the action of wind loading.

In the 1970s and 1980s, the wind pressure coefficient on internal surface of cooling tower was usually simplified as a constant. For example, Diver (1977) considered that the value of internal pressure coefficient was in range between −0.40～−0.50, and Sollenberger *et al*. (1980) suggested that it should be −0.40. Scanlan *et al*. (1982) obtained an internal pressure coefficient of −0.40 from full-scale measurement. Kawarabata *et al*. (1983) believed that internal pressure coefficient in actual design was −0.45. Kasperski *et al*. (1988) found that internal pressure was distributed along the circumferential and height directions, and the internal pressure coefficient was approximately constant −0.50, which was adopted in the design code for cooling tower in German. However, the full-scale measurement of the Maoming cooling tower in Maoming Power Station, Guangdong, China, conducted by Sun *et al*. (1983) showed that internal pressure at the bottom of shell body was non-uniform along the circumferential direction under strong winds. The wind tunnel tests by Li *et al*. (2008) indicated that the uniformity of internal pressure was closely related to the ventilation rate of the packing layer,

*Corresponding author, Professor
E-mail: xuhuihe@csu.edu.cn
** Professor
E-mail: hq.jing@csu.edu.cn
[a] Associate Professor
E-mail: yunfengzou@csu.edu.cn
[b] Ph.D. Student
E-mail: 1624585973@qq.com
[c] Lecturer
E-mail: sylph_li@163.com
[d] Professor
E-mail: iuhw@hnu.edu.cn
[e] Professor
E-mail: zqchen@hnu.edu.cn

ISSN: 1226-6116 (Print), 1598-6225 (Online)

which was installed at the top of the supporting columns. Shen *et al*. (2011a) examined internal pressure distribution using CFD, and they reported that the internal pressure significantly changed along the height and circumferential directions. Bao *et al*. (2009) found a rapid decrease in the internal wind pressure at the bottom wake. Through a wind tunnel test, Shen *et al*. (2011b) found the mean wind pressure acting on the internal surface of the shell depends on both height above ground level z and circumferential angle θ. Ke *et al* (2015) investigated the effects of the radiator shutter ventilation rates on the aerodynamic characteristics of internal wind pressure by Computational Fluid Dynamic (CFD) technology, and found that the drag force coefficient increases with the ventilation rate and reaches the maximum in a building status of full ventilation. Furthermore, Ke *et al*. (2018a, b) investigated action mechanism of internal pressures in straight-cone steel cooling tower under two-way coupling between wind and rain, and the effects of internal pressure on wind-induced responses of cooling tower. In summary, although some researchers considered the internal pressure as a uniform distribution, full-scale measurements, numerical simulations, and wind tunnel tests show that the internal pressure changes along both the height and circumferential positions. No consensus has been reached regarding the distribution features of internal pressure and its values. In addition, most of previous studies were conducted for the cooling towers with the height of approximately 100 m in 1970s to 1990s, while the modern cooling towers have become much higher (Ke *et al*. 2017a, Zhang *et al*. 2017).

In the present study, the hyperbolic cooling tower with height of 220 m in a nuclear station in China is tested in a wind tunnel. The wind pressure coefficients on the internal surface of the cooling tower are obtained by synchronous pressure measurement. The influences of the ventilation rates of the packing layer are considered. The distribution characteristics of internal wind pressure are obtained. Furthermore, the effect of the simplified pressure coefficient constant Cp, simplified θ-constant pressure coefficient $Cp(z)$ and the realistic pressure $Cp(\theta, z)$ on the wind-induced responses are compared.

2. Wind tunnel tests configuration

2.1 Test model

The total height of the prototype cooling tower is 220.00 m and the cooling area is 20,000 m^2, the throat section above ground level is 169.40 m, and the inlet opening above ground level is 13.45 m. The diameters of the top, throat section, and bottom of the shell are 109.00 m, 103.50 m, and 169.90 m, respectively. The shell thickness varies along height z, the minimum shell thickness is 0.23 m at the throat section, whereas the maximum shell thickness is 1.40 m at the lower stiffening ring, which is supported by uniformly distributed 56 pairs of Φ1.4 m X-shaped circular columns.

The experimental model, as Fig. 1 shows, is geometrically similar to the prototype object, and the geometric scale ratio was 1/220 (model height H=1.0 m). The maximum blockage ratio in the wind tunnel is calculated as 4.6%. The shell model is supported by 56 pairs of Φ64 cm X-shaped circular column models, permitting the reproduction of the real draught. The testing model is made of high quality organic glass. The strength and stiffness of the model are sufficient to ensure that no deformation or vibration occur under the wind action during the pressure measuring tests. A total of 504 pressure taps, in 14 levels, are arranged on the internal surface of the model. Each level has 36 measurement points along the circumferential direction with an angular interval of 10°. Fig. 2 presents the layout of the measurement points and the definition of the circumferential angle θ.

The wind pressure on internal surface of cooling tower is closely related to the ventilation rate of the packing layer, which is usually installed at the lower shell edge to cooling water. During construction, the packing layer is not yet installed at the bottom of the tower, therefore, the ventilation rate is set as 100% (completely ventilated). Whereas, during the actual operation, the ventilation rate is usually 30% in China. Therefore, two typical ventilation rates, i.e., 100% and 30%, are considered in this study Fig. 3 shows the homogeneous perforated plate to simulate the packing layer with 30% ventilation rate.

Fig. 1 Test model

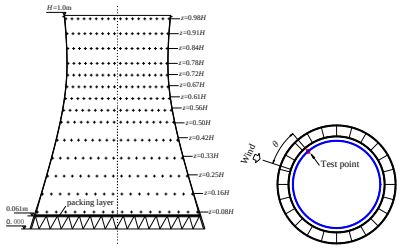

Fig. 2 Pressure taps arrangement and the definition of θ

Fig. 3 homogeneous perforated plate with 30% ventilation rate

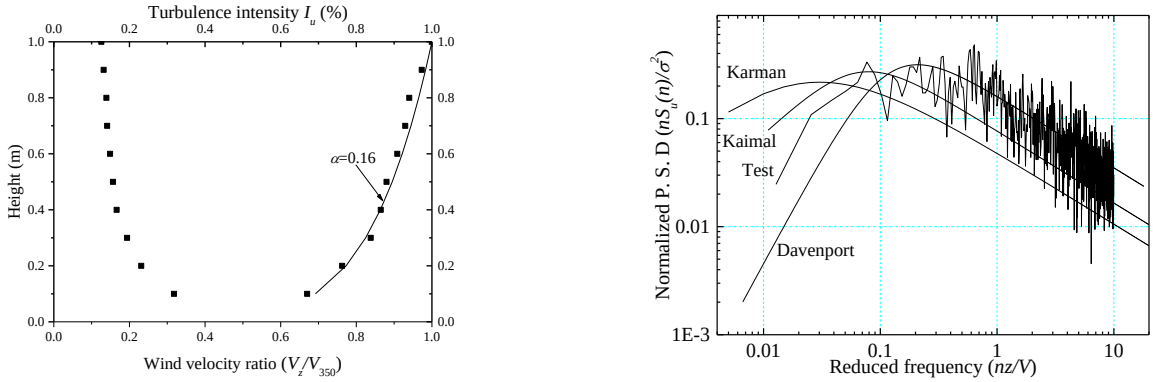

(a) Mean wind speed and turbulence intensity (b) Longitudinal turbulence power spectrum

Fig. 4 Simulation of wind characteristics in BLWT

2.2 BLWT configuration

The wind tunnel test for measuring the internal pressure on the stiff model was conducted at the HD-2 boundary layer wind tunnel (BLWT) in Hunan University, Changsha City, Hunan Province, China. It is a closed-circuit atmospheric boundary layer wind tunnel with two test sections, i.e., the high- and low-speed sections. The high-speed test section is 17.0 m long, 3.0 m wide, and 2.5 m high. The wind speed ranges from 0 to 60 m/s, and the corresponding turbulence intensity (*Ti*) is less than 0.2%. The low-speed test section is 15.0 m long, 5.5 m wide and 4.4 m high. The wind speed ranges of 0 to 18 m/s, with *Ti* of 0.5%. Tests were carried out in turbulent shear flow in the high-speed test section. The "artificial thickening of the boundary layer" was generated with the help of spires at the entrance and irregularities on the floor in the wind tunnel. The flow velocity was measured with a cobra probe anemometer, at the sampling frequency was 2000Hz. The duration of each sample (30 s) was chosen to obtain an error of less than 0.5% on the mean value. The wind characteristics measured at the center of the rotary plate are shown in Fig. 4. The mean wind speed profile is represented by the power law, and profile exponent α=0.16, which corresponds to moderately rough terrain specified in Chinese loading code (GB50009-2012). The turbulence intensity at 100 cm and 77 cm above the floor are 12.5% and 14.0%, which correspond to the top and throat level of the model tower, respectively. As Fig. 4(b) shows, the simulated longitudinal turbulence power spectrum at 50 cm above the floor is consistent with common theoretical spectra, such as those generated by Von Karman, Kaimal and Davenport. In addition, the integral length scale is about 60 cm and corresponded to a full-scale value of 120 m.

2.3 BLWT configuration

A DTC net electronic type pressure scanning system (Pressure Systems, Inc., USA) was employed to measure the wind pressure. In this study, eight modules were used and a total of 512 pressure measuring points monitored simultaneously. For each measurement, the sampling duration lasts 30 s and the sampling frequency was 330 Hz. The pressure taps were linked to the transducers with 600 mm silicon tubes, with an inner diameter of 1.0 mm and an outer diameter of 3.0 mm. The system obtained had flat amplitude and linear variation of the phase up to the sampling frequency, which can guarantee the transmission of the fluctuations without distortions. The free stream oncoming velocity at the top of the model V_H = 18 m/s, corresponding to a Reynolds number of 6.03 × 10^5, based on V_H and the mean diameter of the tower mode. The oncoming flow velocity was monitored using a Pitot tube at the centerline of the test section, about 3 m upstream the tested model.

3. Data processing

To enable the mean data obtained from wind tunnel tests to be applied to prototypes, non-dimensional mean wind pressure coefficient *Cp* is defined as

$$Cp = \frac{\bar{P}(\theta, z) - P_\infty}{\rho V_H^2 / 2} \tag{1}$$

where $\bar{P}(\theta, z)$ is the mean total local pressure on the tower internal surface in (θ, z) coordinates; P_∞ is the static pressure of the undisturbed incoming flow; ρ is the air density, which is usually set to 1.225 kg/m^3; V_H is the free-stream mean velocity at the top of the cooling tower.

For structure with circular cross sections, such as a cooling tower, the mean drag coefficient C_D in the downwind direction can be obtained by area-weighted integral of mean pressure distributions. For a test section with N wind pressure measurement points, the mean drag coefficient C_D can be calculated by

$$C_D = \frac{\sum_{i=1}^{N} C_{Pi} A_i \cos(\theta_i)}{A_T} \tag{2}$$

where A_i is the area for the measurement point i, θ_i is the angle between the ith measurement point and the incoming flow, and A_T is the area of the structure along-wind direction.

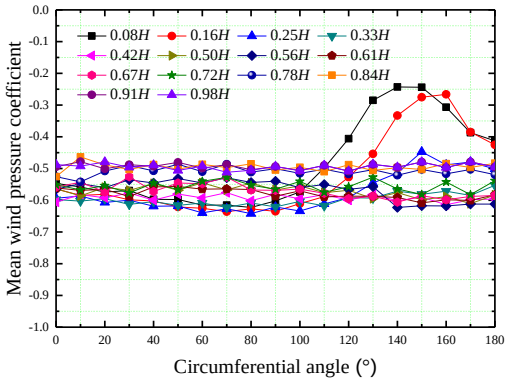

(a) Ventilation rate 100%

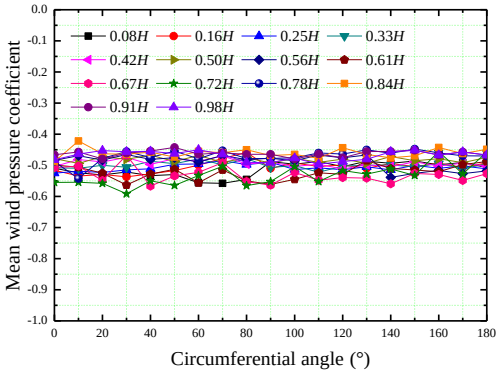

(b) Ventilation rate 30%

Fig. 5 Internal pressure distributions

4. Test results and analysis of wind loading on internal surface

4.1 Mean wind force coefficient

Fig. 5 shows the distribution of measured mean wind pressure on each section along the circumferential direction. Since the cooling tower is the axially symmetrical, and the wind pressure on the internal surface is symmetrically distributed against the incoming wind direction, therefore, only half of the wind pressures (0° to 180°) are presented in this paper. As Fig. 5(a) shows, when the ventilation rate is 100%, the wind pressure at the bottom of the tower shows strong non-uniformity. The pressure coefficient around 150°suddenly increases from −0.55 to −0.24, which is consistent with the results reported by Sun and Zhou (1983). This is because the airflow from the windward side at the bottom of the tower hits the internal wall of the wake flow zone. The average wind pressure coefficients at higher levels show relatively higher uniformity, ranging from −0.50 to −0.60. When the ventilation rate is 30% (Fig. 5(b)), the internal pressure at all levels is uniform along the circumferential direction because of the "rectification" function of the packing layer, which makes the airflow distribution in the tower to be uniform.

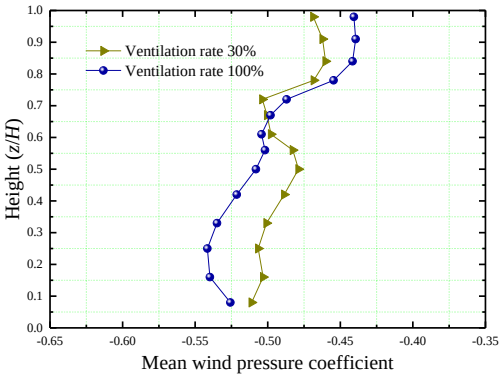

Fig. 6 Mean pressure of measuring layer

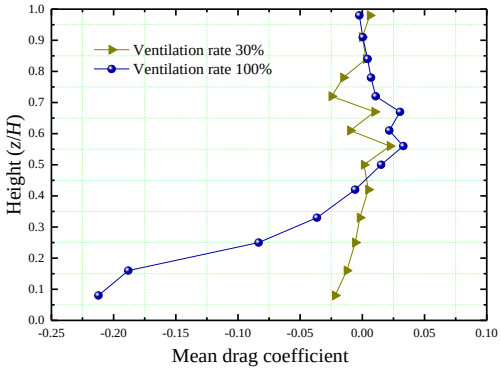

Fig. 7 C_D of measuring layer

However, the distribution of internal pressure is non-uniform along the height direction. Fig. 6 shows the mean pressure coefficient on each measurement layer with respect to height of the test section. It ranges from −0.45 to −0.55. In addition, the ventilation rate of 100% shows stronger non-uniformity than that of 30%. Fig. 7 shows the drag coefficient with respect to height. For the ventilation rate of 100%, the drag coefficient increases from -0.23 to -0.07 as the non-dimensional height increases from 0 to 0.25. When the non-dimensional height is higher than 0.25, the drag coefficient is close to zero. For the ventilation rate of 30%, the drag coefficients in all levels are close to zero, which verifies the uniform distribution of the wind pressure in circumferential direction as shown in Fig. 5(b).

4.2 Turbulence pressure power spectrum

Fig. 8 presents a comparison of the standard power spectra of the fluctuating wind pressures at a typical height and measurement points at different circumferential angles from 0° to 180° when the ventilation rate is 100%. The wind pressure spectra of measurement points 150° and 180° at 0.16 *H* are slightly different at low frequency, because the air enter from the bottom of windward side and flowed to the inside of the tower and hit the inner wall of the wake flow, generating obvious changes in the pulse element of wind speed and flow direction, as well as a re-distribution

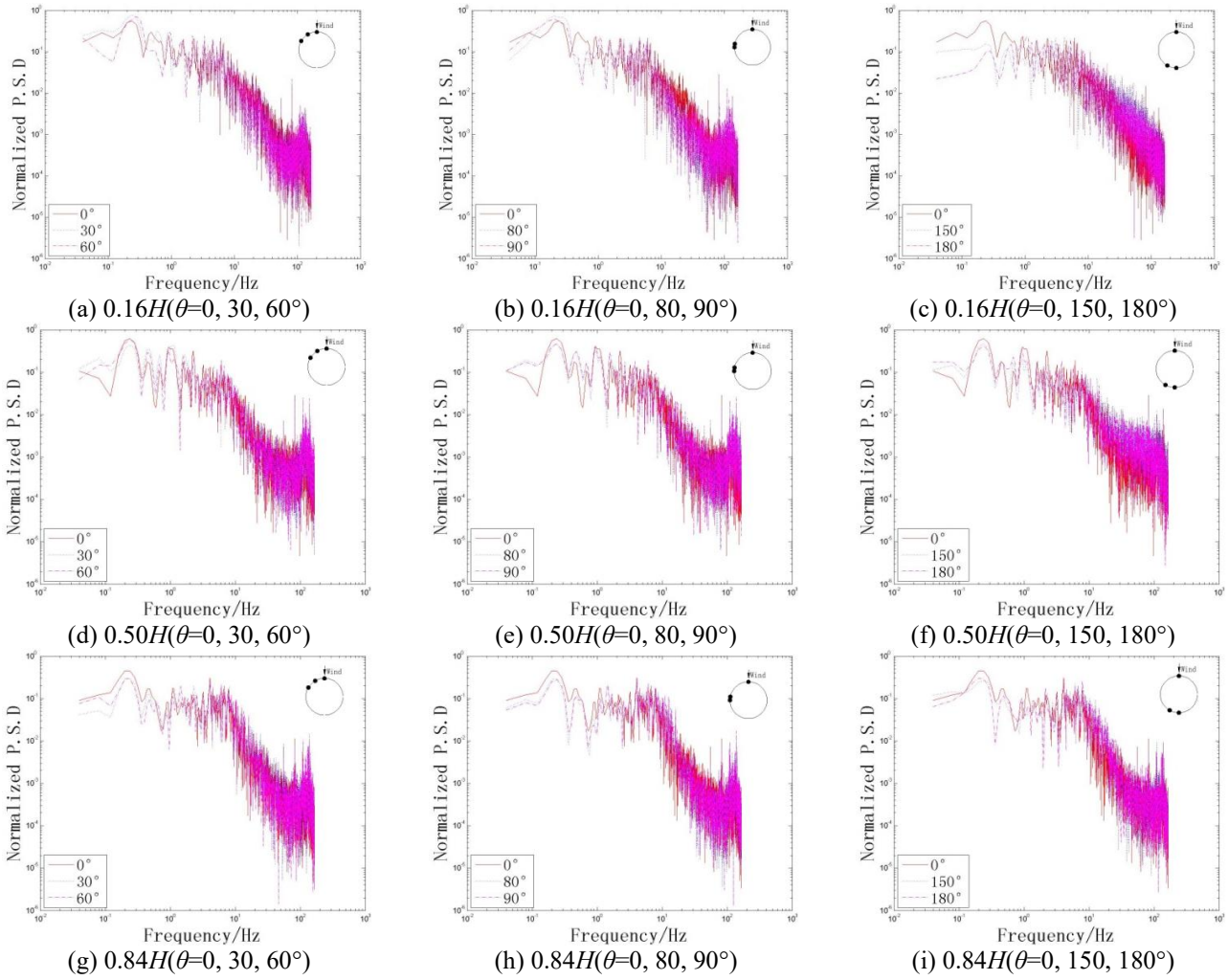

(a) 0.16H(θ=0, 30, 60°) (b) 0.16H(θ=0, 80, 90°) (c) 0.16H(θ=0, 150, 180°)

(d) 0.50H(θ=0, 30, 60°) (e) 0.50H(θ=0, 80, 90°) (f) 0.50H(θ=0, 150, 180°)

(g) 0.84H(θ=0, 30, 60°) (h) 0.84H(θ=0, 80, 90°) (i) 0.84H(θ=0, 150, 180°)

Fig. 8 Turbulence pressure power spectrum results with ventilation rate 100%

of energy. At other measurement levels, the wind pressure spectrum is consistent with that at 0°. In addition, no significant peak is observed.

Fig. 9 shows the standard power spectra of the fluctuating wind pressures at typical heights and measurement points when the ventilation rate is 30%. The power spectrum of the wind pressure at all measurement points is close and no obvious peak appear. This result indicates that the internal flow is stable as a consequence of the rectification of the packing layer at the bottom of the tower.

4.3 Correlation of internal pressure

Fig. 10 shows the correlation coefficients in the circumferential direction using the 0° as a reference point at each test section. In an empty tower (Fig. 10(a), ventilation rate of 100%), the circumferential correlation at the wake flow of the final measurement layer is relatively weak, resulting in a rapid decrease in the circumferential correlation coefficient. The minimum correlation coefficient is approximately 0.1. When the height of the measurement layer is higher than 0.4H the minimum correlation coefficient is higher than 0.6. Since the airflow at the top of the tower enters through a backward flow, the minimum circumferential correlation coefficient is approximately 0.3. When the ventilation rate of the packing layer is reduced to 30% (Fig. 10(b)), the airflow in the tower becomes stable, the circumferential correlation at the bottom measurement point is significantly improved, and the correlation coefficient is higher than 0.8 because of the rectification of the packing layer. However, because of backward flow effect of the airflow, the minimum correlation coefficient is approximately 0.4. In summary, the circumferential correlation distribution of the wind pressure on the internal surface at the middle measurement layer tends to be consistent. That means the circumferential correlation between two measurement points only depend on the circumferential angle. The height of the measurement points have little effects.

Fig. 11 shows the correlation coefficients in the meridian direction using the bottom as a reference point at typical circumferential angle. The results show: (1) the median correlation coefficient obviously decreases within the 0° ~ 90° circumferential angle range in an empty tower (Fig. 11(a)), but the minimum correlation coefficient is still

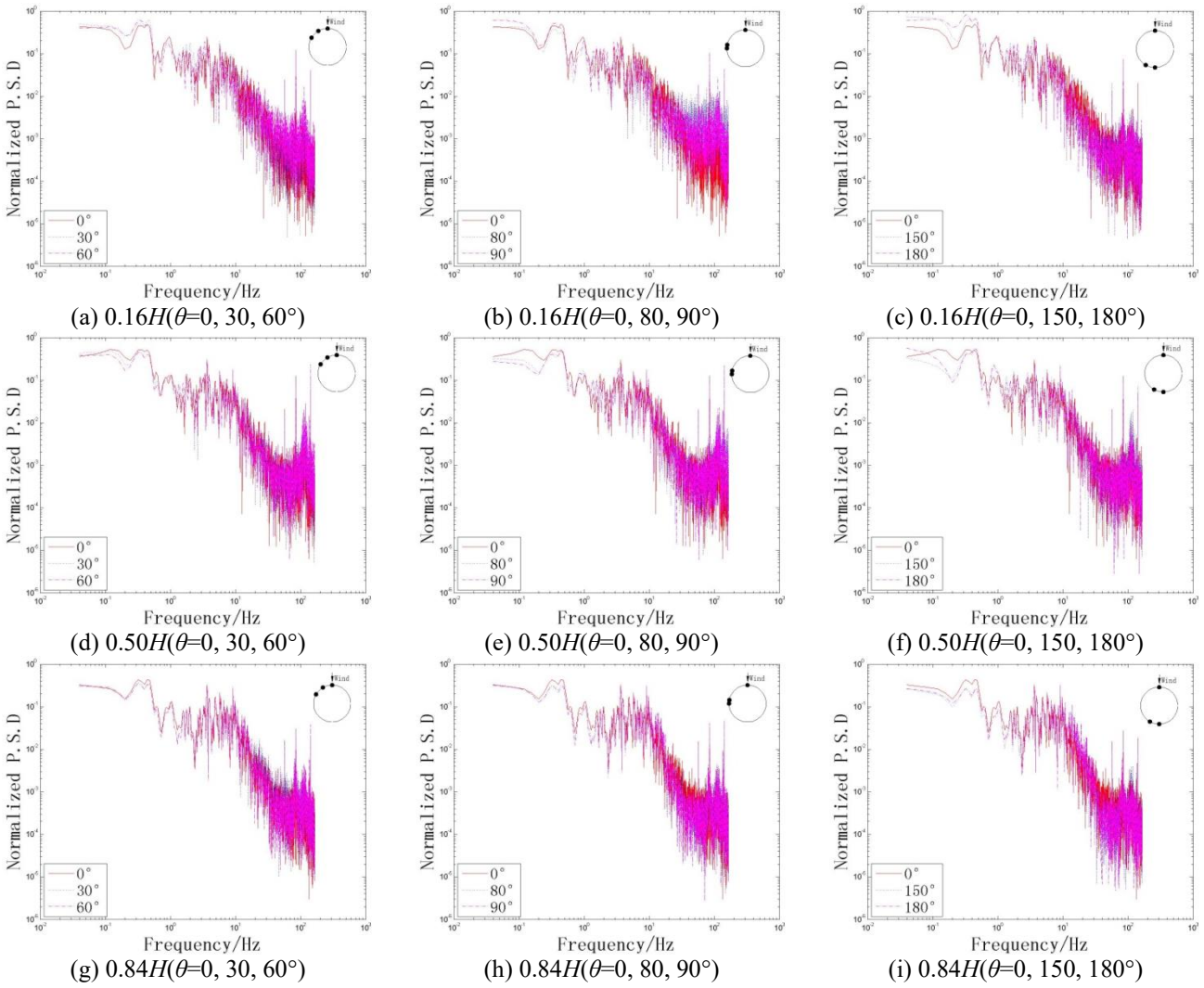

(a) 0.16H(θ=0, 30, 60°) (b) 0.16H(θ=0, 80, 90°) (c) 0.16H(θ=0, 150, 180°)

(d) 0.50H(θ=0, 30, 60°) (e) 0.50H(θ=0, 80, 90°) (f) 0.50H(θ=0, 150, 180°)

(g) 0.84H(θ=0, 30, 60°) (h) 0.84H(θ=0, 80, 90°) (i) 0.84H(θ=0, 150, 180°)

Fig. 9 Turbulence pressure power spectrum results with ventilation rate 30%

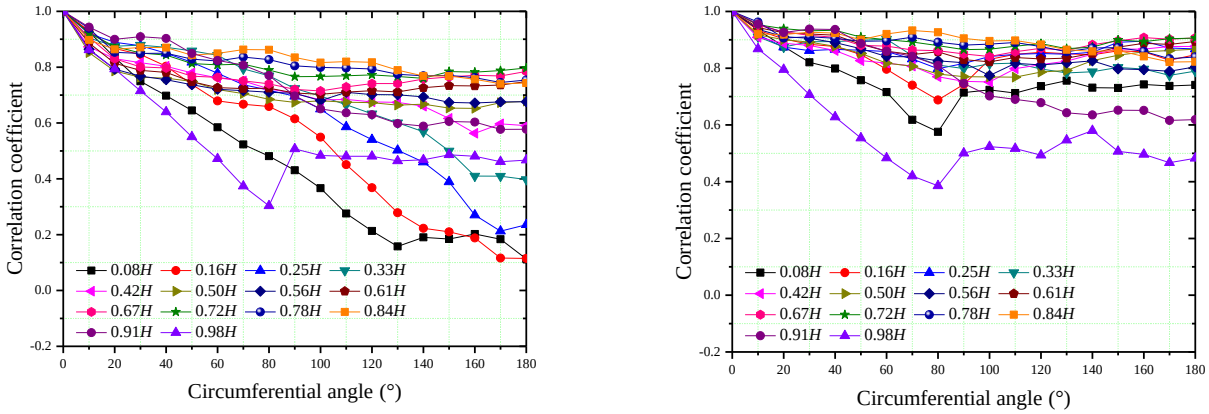

(a) Ventilation rate 100% (b) Ventilation rate 30%

Fig. 10 Correlation of internal pressure in the circumferential direction

higher than 0.2. Beyond the 120°, the median correlation coefficients above the median is consistently 0.1. Given that the air flows from the bottom to the inside of the tower and hits the inner wall of the wake flow, the correlation coefficients between the measurement points in this region and the points at other heights rapidly decrease. As a result of the increase in the circumferential separation between the measurement point and the wake flow zone, the influences

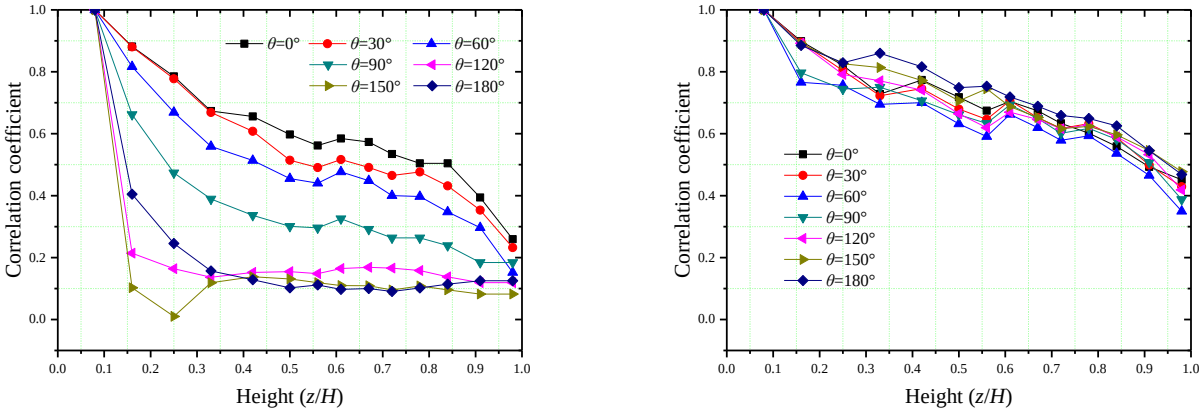

(a) Ventilation rate 100% (b) Ventilation rate 30%

Fig. 11 Correlation of internal pressure in the median direction

of the airflow gradually decrease and thus the median correlation at the measurement point in the windward zone is the strongest. (2) After the packing layer is set at the bottom of the tower (Fig. 11(b)), as a consequence of the rectification by the packing layer, the airflow in the tower becomes stable, the median correlation obviously improves, the minimum correlation coefficient is higher than 0.5, and airflow is not influenced by the circumferential angle, consequently, the median correlation between measurement points is only related to the median height but not the circumferential angle of the measurement points. Generally, as a consequence of the increase in the distance between two measurement points in the median direction, the correlation coefficients gradually decrease, but the wind pressure at each point on a median line is distributed in a positive correlation, because the direction of internal wind pressure all points outwards from the surface.

5. Effect of internal pressure on wind-induced response

5.1 Finite element model and internal pressure values

Analytical model of the 220 m high cooling tower is established by using the finite element software ANSYS. The body of the cooling tower is simulated by using element SHELL63, and the columns are idealized as three-dimensional Timoshenko beams, which are simulated with element BEAM188. Fig. 12 shows the finite-element model and the calculated first-order mode shape. The fundamental frequency f is 0.738 Hz, and there are 4 circular waves and 2 vertical waves in the mode.

In order to compare the influence of different values of internal pressure on wind-induced responses of the cooling tower better, only wind load is considered in the calculation. The internal pressure value in VGB-R 610Ue (2005) is adopted for reference

$$W_I = Cp_I IFq_b(H) \tag{3}$$

where W_I is the equivalent static wind load on the internal surface; Cp_I means the coefficient of the internal wind pressure, which can be calculated by Eq. (1); IF is interference factor to take into account of effect of aerodynamic interference, and a single tower is considered in this calculation, thus, IF=1. Seven cases have been calculated as summarized in Table 1.

The gust wind pressure at the top of the tower is denoted by $q_b(H)$, and $q_b(H)=2.25w_0(H/10)^{0.22}$ is adopt according to VGB-R 610Ue (2005), the basic wind pressure, w_0 is set to 0.45 kPa, which corresponds to the basic wind speed of 26.8 m/s, and the profile exponent 0.22 corresponded to the design code in China (GB50009, 2012).

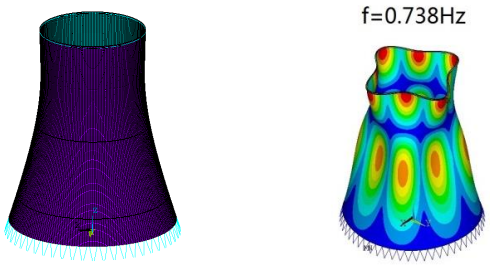

(a) Finite element model (b) First-order modal

Fig. 12 Finite element model and first-order modal

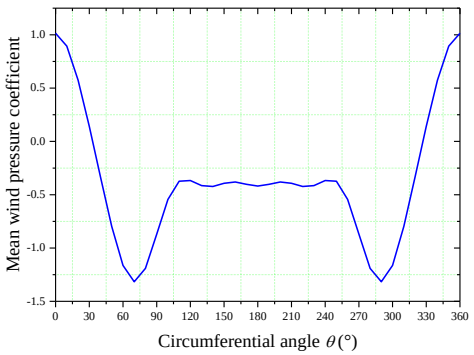

Fig. 13 Wind pressure coefficients distribution on external surface

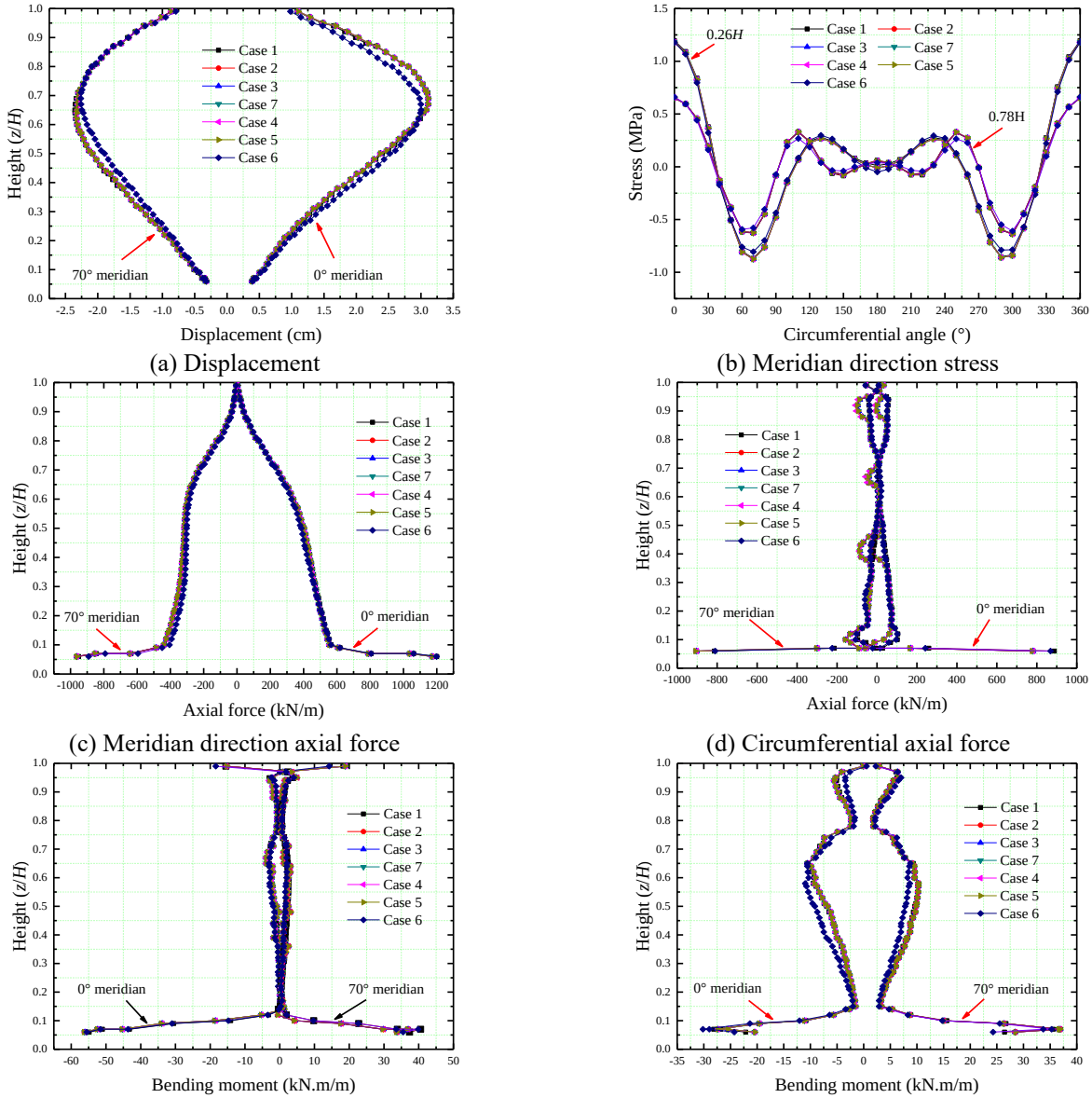

Fig. 14 Wind-induced responses under internal and outer pressure

The wind pressure coefficient on the external surface is compliant with the design codes for the cooling towers in China (GB/T 50102. 2012, NDGJ5-88. 2006), as Fig. 13 shows, which is a simplified height-constant pressure distribution.

5.2 Effect of internal pressure values on static response of the cooling tower

Fig. 14 shows the static responses induced by the external pressure plotted in Fig. 13 and different types of wind loading on internal surface shown in Tab. 1. Since the max responses usually appear in the 0° and 70° meridian directions, the responses in these two directions are selected as examples. It can be seen that the displacement responses due to different types of wind load are close and they are not sensitive to the size and distribution characteristics of the internal pressure. When the distribution of the wind pressure is uneven at the bottom of the tower (i.e., Case 6), the displacement is small. Accordingly, the distribution characteristics of the internal pressure have minimal influence on the internal strain along the meridian direction but have considerable influence on the circumferential strain. The unbalanced distribution of the internal pressure along the meridian direction has a minimal influence on internal strain, but the unbalanced circumferential distribution of the internal pressure has a considerable influence on the internal stain. As a consequence of the unbalanced internal pressure distribution, the internal strain from circumferential pressure is large, whereas the internal strain along the meridian direction is small. Furthermore, the influence of wind pressure at the tower bottom in the circumferential direction on circumferential strain decreases because of an increase in height. When the internal pressure

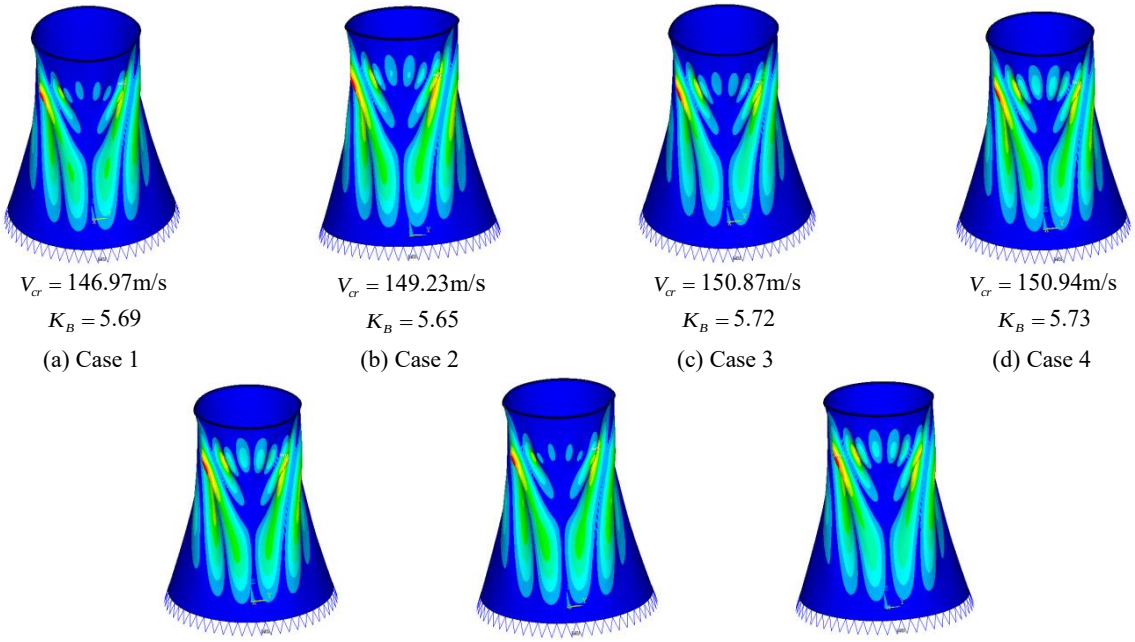

$V_{cr}=146.97$m/s
$K_B=5.69$
(a) Case 1

$V_{cr}=149.23$m/s
$K_B=5.65$
(b) Case 2

$V_{cr}=150.87$m/s
$K_B=5.72$
(c) Case 3

$V_{cr}=150.94$m/s
$K_B=5.73$
(d) Case 4

$V_{cr}=150.34$m/s
$K_B=5.69$
(e) Case 5

$V_{cr}=144.65$m/s
$K_B=5.58$
(f) Case 6

$V_{cr}=150.61$m/s
$K_B=5.82$
(g) Case 7

Fig. 15 Buckling safety of shell

is distributed uniformly, the internal strain from circumferential pressure is directly proportional to the absolute values of internal pressure coefficient but different from pulling strain.

5.3 Effect of internal pressure values on buckling safety of the shell

Stability is one of the essential factors considered in the design of cooling towers. The Chinese design codes have provided the formulas of stability checking for the entire cooling tower and the tower body, respectively. They are

$$q_{cr}=0.052E\left(\frac{h}{r_0}\right)^{2.3} \tag{4}$$

$$0.8K_B\left(\frac{\sigma_1}{\sigma_{cr1}}+\frac{\sigma_2}{\sigma_{cr2}}\right)+0.2K_B^2\left[\left(\frac{\sigma_1}{\sigma_{cr1}}\right)^2+\left(\frac{\sigma_2}{\sigma_{cr2}}\right)^2\right]=1 \tag{5}$$

where q_{cr} is the critical wind pressure; E is the elasticity modulus of concrete; h is the wall thickness at the throat of the cooling tower; r_0 is the diameter at the throat; K_B is the safety factor for elastic buckling; σ_1 and σ_2 refer to the circumferential and meridian pressures, respectively; γ is the Poisson's ratio of concrete; K_1 and K_2 are the parameters determined from the geometric parameters of the tower body; and σ_{cr1} and σ_{cr2} are the critical circumferential and meridian pressures, respectively, which are given by

$$\sigma_{cr1}=\frac{0.985E}{\sqrt[4]{\left(1-\gamma^2\right)^3}}\left(\frac{h}{r_0}\right)^{4/3}K_1 \tag{6a}$$

$$\sigma_{cr2}=\frac{0.612E}{\sqrt[4]{\left(1-\gamma^2\right)^3}}\left(\frac{h}{r_0}\right)^{4/3}K_2 \tag{6b}$$

According to Eq. (4), unstable critical wind speed V_{cr} is calculated as 102.56 m/s by

$$V_{cr}=40\sqrt{q_{cr}} \tag{7}$$

The critical circumferential and meridian pressures, σ_{cr1} and σ_{cr2}, can be calculated by Eq. (6). Accordingly, by substituting the hoop and meridional stresses calculated from ANSYS into Eq. (5), the safety coefficient of the local stability K_B at any point can be obtained.

Fig. 15 shows the calculated results of the buckling stability for the different cases listed in Tab. 1. The buckling mode and minimum local stability safety factors, K_B, are generally consistent. The critical wind speed for the different cases is very close. However, when considering the non-uniformity of the pressure distribution in both directions (Cases 6 and 1), the critical wind speeds are the lowest. When only considering the non-uniformity of the pressure distribution in height direction (Cases 5 and 2), the critical wind speeds are lower but very close to those of Cases 3 and 5. That means the distribution features of the internal pressure have influences on the buckling stability of the cooling tower. The non-uniform distribution in

Table 1 Internal pressure coefficient values and distribution characteristics

Source of value		Method of simplification	Distribution features of internal pressure	Value of internal pressure coefficient	Case No.
Wind tunnel tests	Ventilation rate: 30%	—	Changes along the circumferential and height directions	Fig. 5(b)	Case 1
		Average of the measurement points in the circumferential direction	Does not change along the circumferential direction but changes along the height direction	Fig. 6	Case 2
		Average of all testing points	Does not change along the circumferential and height directions	−0.49	Case 3
	Ventilation rate: 100%	Average of the testing points in the circumferential direction	Does not change along the circumferential direction but changes along the height direction	Fig. 6	Case 4
		Average of all testing points	Does not change along the circumferential direction but changes along the height direction	−0.52	Case 5
		—	Changes along the circumferential and height directions	Fig. 5(a)	Case 6
German standards		—	Does not change along the circumferential and height directions	−0.50	Case 7

Note: "—" means non-simplified method was adopted.

circumferential direction have more influence than those in height direction. In addition, when the internal pressure is uniform, the critical wind speeds are inversely proportional to the absolute values of the internal pressure, i.e., the buckling safety is reduced by higher suction pressure. All critical wind speeds derived from ANSYS are higher than 102.56 m/s that calculated by Eq. (7).

According to the calculation results of the static responses and buckling stability, even though the internal pressure coefficient of the cooling tower varies along the height and circumferential directions, a simplified constant -0.50 can get very close results. Besides, the calculated critical wind speed from Eq. (7) is most conservative and should be the key parameter to guarantee the safety of the tower.

5.4 Effect mechanism of internal pressure on wind-induced response

To further analyze the influence mechanism of the internal pressure values and the distribution features on the wind-induced response, the static responses of the cooling tower under only the internal pressures listed in Table 1 are calculated and shown in Fig. 16. The results show that the responses increase when the wind pressure is non-uniform along the circumferential direction at the tower bottom (Case 6 has the largest responses). The responses are relatively small compared with that considering external pressure listed in Fig. 14. The maximum displacement induced by the internal pressure in Fig. 16 is approximately 0.25 cm, less than 10% of the displacement due to the external pressure. Consequently, although the value and distribution features of the internal pressure have certain influences on the wind-induced response of the cooling tower, it is much smaller compared with those of the external pressure. Simplifying the internal pressure with **"**3D effect**"** as a constant distribution along the height and circumferential directions can satisfy the safety requirement of the cooling tower.

6. Conclusions

In the present study, the wind pressure on the internal surface on a stiff cooling tower model are measured by wind tunnel test. Two typical cases with the ventilation rates of 100% and 30%, representing the construction and operation states, respectively, have been tested. The effects of the non-uniformity of the internal wind pressure along the height and circumferential directions on the static responses and buckling stability of the cooling tower are investigated through a finite-element method. The main conclusions are drawn as following.

- The wind pressure on the internal surface of the cooling tower is closely related to the ventilation rate of the packing layer at the tower bottom. The rectification action of the packing layer makes the airflow distribution more uniform in the tower, and enhances the correlation of the

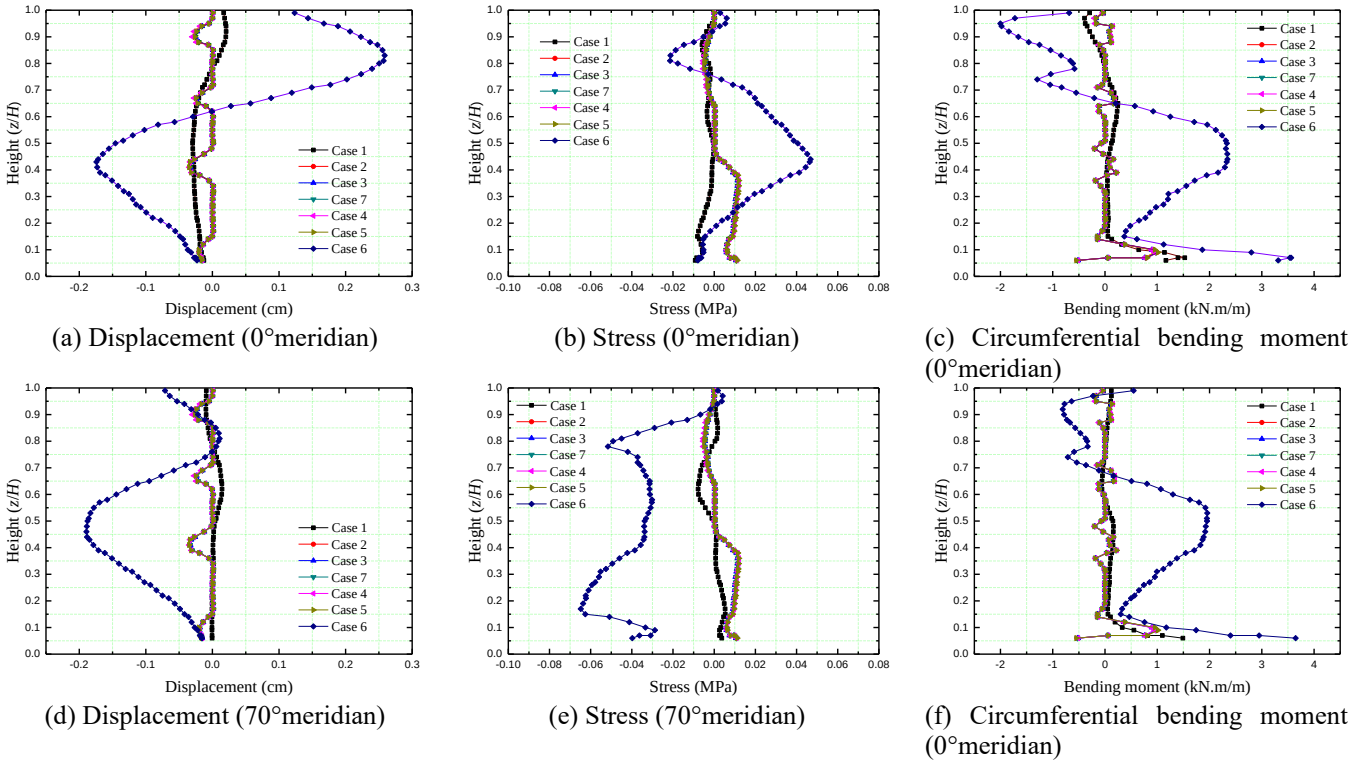

(a) Displacement (0°meridian) (b) Stress (0°meridian) (c) Circumferential bending moment (0°meridian)

(d) Displacement (70°meridian) (e) Stress (70°meridian) (f) Circumferential bending moment (0°meridian)

Fig. 16 Wind-induced responses due to different internal pressures

wind pressure in the circumferential and median directions.

- The wind pressure on the internal surface is non-uniformly distributed along both height and circumferential directions, and the circumferential unbalance is mainly ascribed to the bottom wind pressure during construction.
- The distribution features of internal pressure have influence in the wind-induced response of cooling tower. The non-uniformity in circumferential direction has more effect than that in height direction.
- For a 220 m high cooling tower, a constant internal pressure of -0.5 can well prediction the critical wind speed when considering the static responses and buckling stability.

Acknowledgments

The work presented in this paper was supported by grants received from the National Natural Science Foundations of China (Project Nos. 51508580, U1534206 and 51508574), and National Key R&D Program of China (Project No. 2017YFB1201204). Natural Science Foundations of Hunan Province (Project No. 2016JJ3149) is also gratefully acknowledged.

References

Bamu, P.C. and Zingoni, A. (2005), "Damage, deterioration and long-term structural performance of cooling-tower shells: A survey of developments over the past 50 years", *J. Eng. Struct.*, **27**, 1794-1800. https://doi.org/10.1016/j.engstruct.2005.04.020.

Bao, K.Y., Shen, G.H. and Sun, B.N. (2009), "Numerical simulation of mean wind load on large hyperbolic cooling tower", *Acta Aerod. Sinica*, **27**(6), 650-655. (in Chinese)

C. E. G. B. (1965), "Report of the committee of inquiry into the collapse of cooling towers at Ferrybridge on November 7, 1965", *UK: Central Electricity Generating Board*. https://trove.nla.gov.au/version/25162701.

Cheng, X.X., Zhao, L., Ge, Y.J., Dong, J. and Demaritino, C. (2017), "A comprehensive high Reynolds number effects simulation method for wind pressures on cooling tower models", *Wind Struct.*, **24**(2), 119-144. https://doi.org/10.12989/was.2017.24.2.119.

Diver, M. (1977), "Large cooling towers the present trend", *J. Struct.Engineer*, **10**(55), 130-137.

Hashish, M.G. and Abu-Sitta, S.H. (1974), "Response of hyperbolic cooling towers to turbulent wind", *J. Struct. Eng.*, **100**(5), 1037-1051.

Harnach, R. and Niemann, H.J. (1980), "The influence of realistic mean wind loads on the static response and the design of high cooling towers", *Eng. Struct.*, **2**, 27-34. https://doi.org/10.1016/0141-0296(80)90026-7.

Kawarabata, Y., Nakae, S. and Harada, M. (1983), "Some aspects of the wind design of cooling towers", *J. Wind Eng. Ind. Aerod.*, **14**, 167-180. https://doi.org/10.1016/0167-6105(83)90020-X.

Kasperski, M. and Niemann, H.J. (1988), "On the correlation of dynamic wind loads and structural response of natural-draught cooling towers", *J. Wind Eng. Ind. Aerod.*, **30**(2), 67-75. https://doi.org/10.1016/0167-6105(88)90072-4.

Ke, S.T., Ge, Y.J. and Zhao, L. (2012), "A new methodology for analysis of equivalent static wind loads on super-large cooling towers". *J. Wind Eng. Ind. Aerod.*, **111**, 30-39. https://doi.org/10.1016/j.jweia.2012.08.001.

Ke, S.T., Liang, J., Zhao, L. and Ge, Y.J. (2015), "Influence of ventilation rate on the aerodynamic interference between two extra-large indirect dry cooling towers by CFD", *Wind Struct.*, **20**(3), 449-468. http://dx.doi.org/10.12989/was.2015.20.3.449.

Ke, S.T., Wang, H. and Ge, Y.J. (2017a), "Multi-dimensional extreme aerodynamic load calculation in super-large cooling towers under typical four-tower arrangements", *Wind Struct.*, **25**(2), 101-129. http://dx.doi.org/10.12989/was.2017.25.2.101.

Ke, S.T., Wang, H. and Ge, Y.J. (2017b), "A study on the average wind load characteristics and wind-induced responses of a super-large straight-cone steel cooling tower", *Wind Struct.*, **25**(5), 91-109. http://dx.doi.org/10.12989/was.2017.25.5.433.

Ke, S.T., Du, L.Y., Ge, Y.J., Yang, Q., Wang, H. and Tamura, Y. (2018a), "A study on the action mechanism of internal pressures in straight-cone steel cooling tower under two-way coupling between wind and rain". *Wind Struct.*, **27**(1), 65-74. http://dx.doi.org/10.12989/was.2018.27.1.011.

Ke, S.T, Du, L.Y., Ge, Y.J. and Tamura, Y. (2018b), "Multi-dimensional wind vibration coefficients under suction for ultra-large cooling towers considering ventilation rates of louvers", *Struct. Eng. Mech.*, **66**(2), 14-21. https://doi.org/10.12989/sem.2018.66.2.273.

Karakas, A, Ozgan, K. and Daloglu, A.T. (2016), "A consistent FEM-Vlasov model for hyperbolic cooling towers on layered soil under unsymmetrical wind load", *Wind Struct.*, **22**(6), 617-633. http://dx.doi.org/10.12989/was.2016.22.6.617.

Li, P.F., Zhao, L. and Ge, Y.J. (2008), "Investigation on wind load characteristics for super large cooling tower in wind tunnel", *Eng. Mech.*, **25**(6), 60-67. (in Chinese)

Ministry of construction of the people's Republic of China, GB/T 50102-2003 (2003), "Code for design of cooling for industrial recalculating water". *Beijing, China Planning Press*.

Nimeann, H.J. and Zerna, W. (1986), "Impact of research on development of large cooling towers", *J. Eng. Struct.*, **8**, 74-86. https://doi.org/10.1016/0141-0296(86)90023-4.

People's Republic of China Ministry of Construction, GB50009-2012 (2012), "Load code for the design of building structures", *Beijing, China Building Industry Press*, (in Chinese)

Sollenberger, N.J. and Billington, D.P. (1980), "Wind loading and response of cooling towers", *J. Struct. Div. - ASCE*, **103**(3), 601-621.

Scanlan, R.H. and Leonard, J.F. (1982), "Turbulent winds and pressure effects around a rough cylinder at high Reynolds number", *J. Wind Eng. Ind. Aerod.*, **9**, 207-236. https://doi.org/10.1016/0167-6105(82)90016-2.

Shen, G.H., Zhang, C.S. and Sun, B.N. (2011a), "Numerical simulation of wind load on inner surface of large hyperbolic cooling tower", *J. Harbin Inst. Technol.*, **43**(4), 104-108. (in Chinese)

Shen, G.H., Yu, G.P. and Sun, B.N. (2011b), "Analysis of wind load on large hyperbolic cooling tower considering interaction between internal and external pressure", *Acta Aerod. Sinica*, **29**(4), 339-446. (in Chinese)

Sun, T.F. and Zhou, L.M. (1983), "Wind pressure distribution around a ribless hyperbolic cooling tower", *J. Wind Eng. Ind. Aerod.*, **14**(1-3), 181-192. https://doi.org/10.1016/0167-6105(83)90021-1.

Technical Guideline for the Structural Design, Computation and Execution of Cooling Towers (2005), *Structural Design of Cooling Towers(VGB-R 610Ue)*. German.

The people's Republic of China National Development and Reform Commission, NDGJ5-88 (2006), "Technical specification for hydraulic design of thermal power plant". *Beijing: China Electric Power Press*, (in Chinese).

Zhao, L. and Ge, Y.J. (2010), "Wind loading characteristics of super-large cooling towers", *Wind Struct.*, **13**(3), 257-273.

Zhao, L., Ge, Y.J. and Kareem, A. (2017), "Fluctuating wind pressure distribution around full-scale cooling towers", *J. Wind Eng. Ind. Aerod.*, **165**, 34-45. https://doi.org/10.1016/j.jweia.2017.02.016.

Zou, Y.F., He, X.H., Jing, H.Q., Zhou, S., Niu, H.W. and Chen, Z.Q. (2018), "Characteristics of wind-induced displacement of super-large cooling tower based-on continuous medium wind tunnel test", *J. Wind Eng. Ind. Aerod.*, **180**, 201-212. https://doi.org/10.1016/j.jweia.2018.08.001.

Zhang, J.F., Ge, Y.J. and Zhao, L. (2013), "Influence of latitude wind pressure distribution on the responses of hyperbolodial cooling tower shell", *Wind Struct.*, **16**(6), 579-601. http://dx.doi.org/10.12989/was.2013.16.6.579.

Zhang, J.F., Ge, Y.J., Zhao, L. and Zhu, B. (2017), "Wind induced dynamic responses on hyperbolic cooling tower shells and the equivalent static wind load", *J. Wind Eng. Ind. Aerod.*, **169**, 280-289. https://doi.org/10.1016/j.jweia.2017.08.002.

CC